

## 3D imaging of geofluid by wideband magnetotellurics

OGAWA, Yasuo<sup>1\*</sup> ; ICHIKI, Masahiro<sup>2</sup> ; KANDA, Wataru<sup>1</sup>

<sup>1</sup>Volcanic Fluid Research Center, Tokyo Institute of Technology, <sup>2</sup>Graduate School of Science, Tohoku University

Magnetotelluric measurements have been conducted over the five years in the central part of NE Japan arc surrounding the Naruko Volcano with approximately 3km grid. Over 200 sites were used for modeling the crustal resistivity structure in detail. Full impedance tensors for 8 periods were used for inversion. To alleviate the computational load, first four short periods were used to image upper crustal features and the resultant model was used for a prior model for another set of inversions with longer 4 periods.

The obtained model show the crustal conductor underneath the Mukaimachi caldera and Sanzugawa caldera. Seismic tomography shows low S-wave velocity for both, however, the resistivity image show clear low resistivity for Mukaimachi Caldera, but not for Sanzugawa Caldera. This difference may be due to the salinity of the fluids underlying the volcanic regions.

Keywords: geofluid, magnetotellurics, resistivity, 3d

## Three dimensional electrical conductivity model in the subduction zone beneath north-eastern Japan

ICHIKI, Masahiro<sup>1\*</sup> ; OGAWA, Yasuo<sup>2</sup> ; KAIDA, Toshiki<sup>1</sup> ; DEMACHI, Tomotsugu<sup>1</sup> ; HIRAHARA, Satoshi<sup>1</sup> ; HONKURA, Yoshimori<sup>2</sup> ; ICHIHARA, Hiroshi<sup>3</sup> ; KANDA, Wataru<sup>2</sup> ; KONO, Toshio<sup>1</sup> ; KOYAMA, Takao<sup>4</sup> ; MATSUSHIMA, Masaki<sup>5</sup> ; NAKAYAMA, Takashi<sup>1</sup> ; SUZUKI, Shu'ichi<sup>1</sup> ; TOH, Hiroaki<sup>6</sup> ; UYESHIMA, Makoto<sup>4</sup>

<sup>1</sup>Grad. School of Sci., Tohoku University, <sup>2</sup>VFRC, Tokyo Institute of Technology, <sup>3</sup>IFREE, JAMSTEC, <sup>4</sup>ERI, The University of Tokyo, <sup>5</sup>Grad. School of Sci. & Eng., Tokyo Tech, <sup>6</sup>Grad. School of Sci., Kyoto University

Our final goal is to infer a geofluid map (GFM) from both of the seismological (seismic velocity,  $V_p/V_s$ ,  $Q$  etc.) and electrical conductivity structures in the wedge mantle of subduction zone beneath northeastern Japan. While plenty of high-resolution three dimensional (3-D) seismic tomographic images has been revealed there, none of 3-D electrical conductivity distribution model, of which the resolution is comparative to those of seismic tomography, has been proposed in terms of wedge mantle in subduction zones. Here, we show a high-resolution 3-D electrical conductivity distribution model in the wedge mantle beneath northeastern Japan used as input of GFM.

We carried out long-period MT observation using the state-of-the-art equipments, LEMI-417 and NIMS. The total 72 site observation has been completed. To remove tilt changes, baseline steps and drifts of fluxgate magnetometers, we first subtracted magnetic field variations to which a median filter was applied, from raw data. The horizontal coordinate of magnetic field data in each site was rotated before the response calculation such that the declination of the averaged horizontal component should be consistent with the 2010 absolute geomagnetic observation map provided by Geospatial Information Authority of Japan. We used the BIRRP processing code (Chave and Thomson, 2004) to estimate MT responses and have successfully retrieved them up to 61440 seconds in period.

The MT impedance responses were inverted into 3-D electrical conductivity model using WSINV3D (Siripunvaraporn et al, 2005), the data-space Occam inversion method. The all input data error floor was assigned to be 10 percent. We investigated the optimal reference model with trial and errors. The test model was (1) uniform models, (2) layered models and (3) layered models with subducting slab models. The best RMS in each reference model was (1) 2.81, (2) 2.71 and (3) 2.48, respectively. Hence, we adopted the reference model of the layered model with subducting slab.

The conductivity profiles normal to the trench axis in higher latitude than N 39 degrees delineate conductive region on the subducting slab, and the conductive region is raised just beneath the central range of northeastern Japan (Ou-backbone range). This electrical image is well consistent with that obtained by the seismic tomographic model. On the other hand, a profile in lower latitude than N 39 degrees reveals that the conductive region is overturned towards backarc. The top of the overturned conductive body coincides with Gassan Volcano location, one of the outstanding backarc volcanism. However, Chokai Volcano, another distinctive backarc volcanism has no subsurface conductive root originated from deep upper mantle. The overturned mantle convection image is not found in the seismic tomographic image.

## S-wave attenuation on the western side of Nankai subduction zone: implications for geofluid distribution and dynamics

TAKAHASHI, Tsutomu<sup>1\*</sup> ; OBANA, Koichiro<sup>1</sup> ; YAMAMOTO, Yojiro<sup>1</sup> ; NAKANISHI, Ayako<sup>1</sup> ; KODAIRA, Shuichi<sup>1</sup> ; KANEDA, Yoshiyuki<sup>1</sup>

<sup>1</sup>JAMSTEC

One major cause of seismic wave attenuation is the presence of fluid in rocks. In this study, we estimated the attenuation structure in southwestern Japan and western Nankai trough by applying the attenuation tomography that takes account of apparent amplitude attenuation due to multiple forward scattering [Takahashi, 2012]. Because the estimated attenuation  $1/Q$  in our tomographic study was much larger than  $1/Q$  due to wide-angle scattering, our estimated  $1/Q$  is composed mainly the intrinsic  $1/Q$ .

High  $1/Q$  ( $>1/500$  at 4-8 Hz) was imaged beneath the Quaternary volcanoes. The highest attenuation ( $1/Q \sim 1/250$  at 4-8 Hz) distributes beneath the Beppu-Shimabara rift zone at 40-60km depth. Beneath this rift zone,  $1/Q$  becomes larger as depth increases. Random inhomogeneities in this zone are relatively strong at 0-40 km depth; whereas at 40-60 km depth random inhomogeneities are almost comparable to those in non-volcanic area. Meanwhile, in northeastern Japan, uppermost mantle beneath the volcanoes shows strong inhomogeneities and high attenuation. Apparent attenuation at the uppermost mantle beneath the Quaternary volcanoes is high in both study areas, but relative contributions of scattering and intrinsic attenuation differ between northeastern Japan and the Beppu-Shimabara rift zone. If we consider random inhomogeneities and  $1/Q$  in other areas, the weak random inhomogeneities and high  $1/Q$  beneath this rift zone suggest that random inhomogeneities due to the presence of igneous rocks are not significant, and that any magma inclusions are too small to excite S-wave scattering at 4-32 Hz.

At off Shikoku region, moderate  $1/Q$  ( $1/800 \sim 1/1000$  at 4-8 Hz) is imaged at 0-20 km depth. This moderate  $1/Q$  is estimated as  $1/Q(f) \sim 10^{-2.5} f^{-0.5}$ . Similar moderate attenuation can be found beneath the south of Shikoku at 20-40km, beneath the northern edge of Shikoku at 40-60km depth, and beneath Chugoku area at 40-60km depth. From geometry models of subducting Philippine Sea plate, most of the moderate  $1/Q$  zone is located in and around the oceanic crust of subducting Philippine Sea plate except beneath Chugoku region. In this area, Shelly et al. [2006] pointed out fluid existence in the oceanic crust by estimating  $V_p/V_s$  structure. This correspondence implies this moderate  $1/Q$  reflects fluid in the subducting slab. If we suppose that  $1/Q$  of P- and S-wave have the same frequency dependences and that random inhomogeneities of P- and S-wave has the same scale dependences, we can show possible cases of fluid flow induced by the passage of low frequency seismic waves ( $<1$  Hz) by applying a theoretical model of wave attenuation in saturated porous random media [Muller and Gurevich, 2005]. As a phenomenon suggesting such fluid flow by lower frequency seismic wave, triggering of non-volcanic tremors by surface waves passing has been observed [e.g., Miyazawa and Brodsky, 2008]. Even though we further need P-wave studies for detailed examination of this topic, it is likely that random inhomogeneity, intrinsic at 4-32 Hz and triggered tremors can be used to investigate medium properties and fluid dynamics.

## Seismic activity near the Moriyoshi-zan volcano in northeastern Japan: Implications for geofluid migration

KOSUGA, Masahiro<sup>1\*</sup>

<sup>1</sup>Graduate School of Science and Technology

The 2011 Off the Pacific coast of Tohoku (Tohoku-oki) Earthquake caused increased seismicity in many inland areas. A seismic cluster that occurred north of the Moriyoshi-zan volcano in the Akita prefecture of the Tohoku District is of interest in light of contribution of geofluids to seismic activity. We observed a seismic cluster characterized by the migration of seismicity, reflected/scattered phases, and deep low-frequency earthquakes. We relocated hypocenters by using the data of temporal observation and by using the Double-Difference location technique, which increased the depth accuracy. We interpreted the spatiotemporal variation of the hypocenters in the most active cluster by estimating the migration of pore fluid pressure. The hydraulic diffusivity of the cluster was in the range of 0.01-1.0 m<sup>2</sup>/s, and increased with time, implying that the migration of hypocenters accelerated after a pathway for fluids was formed by the fracturing of the wallrock that produced the initial stage of seismic activity. A prominent feature of the seismograms is a reflected/scattered phase observed at stations around the volcano. We have interpreted the phase as S-to-S scattered waves and estimated the location of scatterers using a back-projection method. The scatterers are located about 5 km northwest of the Moriyoshi-zan volcano and at an approximate depth of 13 km. The Moriyoshi-zan area is one of the source areas of deep low-frequency earthquakes that have previously been interpreted as events generated by the migration of geofluids. The depth of scatterers is close to the upper limit of the depth at which low-frequency earthquakes occur. Thus, we regard the observed scatterers to be a reservoir of geofluid that came from the uppermost mantle accompanying contemporaneous low-frequency earthquakes. The geofluid reservoir is the probable source of overpressurized fluid that induces the migration of seismicity in the upper crust. A time delay in seismic activity from the Tohoku-oki Earthquake was considered as the time needed to migrate across a gap between the reservoir and the earthquake cluster with a hydraulic diffusivity comparable to that observed for the initial stage of seismicity, i.e., fracturing of the wallrock.

Keywords: The 2011 Off the Pacific coast of Tohoku Earthquake, triggered seismicity, hypocenter migration, scattering, geofluid

## Is H<sub>2</sub>O-NaCl fluid enough to explain high electrical conductivity in the earth's crust?

SAKUMA, Hiroshi<sup>1\*</sup> ; ICHIKI, Masahiro<sup>2</sup>

<sup>1</sup>National Institute for Materials Science, <sup>2</sup>Tohoku University

Old continental crust has a high electrical conductivity layer at 20 to 30 km in depth [1]. Presence of aqueous fluids is a plausible hypothesis for explaining the high conductivity zone [2]. Therefore the electrical conductivities of aqueous fluids under high pressure ( $P$ ), temperature ( $T$ ) conditions should be investigated in order to evaluate the hypothesis. The phases of water and aqueous NaCl solutions at the  $P$ - $T$  conditions of the Earth's crust correspond from liquid to supercritical states.

Experimental approaches to measure the electrical conductivities at high  $P$ ,  $T$  and salt concentration ( $c$ ) conditions are limited and the data at  $P < 400$  MPa,  $T < 1073$  K and  $c < 0.6$  wt% for aqueous NaCl solutions is only available [3]. Classical molecular dynamics (MD) simulations are useful to obtain the electric conductivities at high  $P$ ,  $T$  and  $c$  conditions and for understanding the underlying mechanism controlling the conductivities.

We used the flexible and induced point charge (FIPC) H<sub>2</sub>O model [4] for MD simulations of aqueous NaCl solution. The technical details of the model and computational methods are explained in the literature [4]. The unit cell contained 2222 H<sub>2</sub>O and 4 NaCl, 2035 H<sub>2</sub>O and 22 NaCl, and 2035 H<sub>2</sub>O and 66 NaCl for  $c = 0.6, 3.4,$  and  $9.6$  wt% NaCl solutions, respectively.

The isotherms indicate that the conductivity increases with increasing pressures and saturated at high pressures. The conductivity decreased with increasing temperature. This behavior may seem to be strange, since the ionic mobility should be high at high temperatures. This can be explained by the mixed effects of the change of (i) the density, (ii) ionic mobility, and (iii) dielectric constant of water as discussed in Quist and Marshall (1968) [3]. We concluded that the change of the conductivity of H<sub>2</sub>O-NaCl fluids along with a geotherm model can explain one order of the increased magnitude at the high conductivity layer in depth, but more change observed by the Magnetotelluric method should be explained by the additional mechanism such as the connectivity of the fluids and the conductivity of H<sub>2</sub>O-CO<sub>2</sub> fluids.

### References

- [1] T. J. Shankland and M. E. Ander (1983) *J. Geophys. Res.* **88** 9475-9484.
- [2] B. E. Nesbitt (1993) *J. Geophys. Res.* **98** 4301-4310.
- [3] A. S. Quist, and W. L. Marshall, (1968) *J. Phys. Chem.* **72** 684-703.
- [4] H. Sakuma, M. Ichiki, K. Kawamura and K. Fuji-ta (2013) *J. Chem. Phys.* **138** 134506.

Keywords: salt water, electrical resistivity, supercritical fluid, molecular dynamics, static dielectric constant

## Connectivity of cracks and pores in a granitic rock

WATANABE, Tohru<sup>1\*</sup> ; HIGUCHI, Akiyoshi<sup>1</sup> ; YONEDA, Akira<sup>2</sup>

<sup>1</sup>Graduate school of science and engineering, University of Toyama, <sup>2</sup>Institute for Study of Earth's Interior, Okayama University

Seismic velocity and electrical conductivity are used to map the fluid distribution in the crust. Seismic velocity reflects the contiguity of solid phases, while electrical conductivity the connectivity of fluid phases. The combination of velocity and conductivity could provide us a strong constraint on the fluid distribution. However, mapping of the fluid distribution has not been successful. The connectivity of fluid phases in rocks is poorly understood. In order to understand the connectivity of fluid phases in rocks, we have made conductivity measurements on a fluid-bearing granitic rock under various confining pressures.

Fine grained (100-500 $\mu$ m) biotite granite (Aji, Kagawa pref., Japan) was used as a rock sample. The sample is composed of 52.8% plagioclase, 36.0% Quartz, 3.0% K-feldspar, 8.2% biotite. The density is 2.66(1) g/cm<sup>3</sup>, and the porosity 0.8(1) %. The porosity was estimated from the mass of the dry and wet samples. Cylindrical samples have dimensions of 25 mm in diameter and 30 mm in length, and saturated with 0.01 mol/l KCl aqueous solution. Simultaneous measurements of elastic wave velocity and electrical conductivity were made using a 200 MPa hydrostatic pressure vessel. The pore-fluid is electrically insulated from the metal work by using plastic devices (Watanabe and Higuchi, 2013). The confining pressure was progressively increased up to 125 MPa, while the pore-fluid pressure was kept at 0.1 MPa. It took five days or longer for the electrical conductivity to become stationary after increasing the confining pressure.

Elastic wave velocities and electrical conductivity showed reproducibly contrasting changes for a small increase in the confining pressure. Elastic wave velocities increased only by 5% as the confining pressure increased from 0.1 MPa to 25 MPa, while electrical conductivity decreased by an order of magnitude. The increase in velocities is caused by the closure of cracks. Most (~80%) of the decrease in electrical conductivity occurred below the confining pressure of 5 MPa. The decrease in electrical conductivity must also be caused by the closure of cracks. The decrease in porosity was only 0.07(1) %. Such a small change in porosity caused a large change in electrical conductivity. The connectivity of fluid was maintained at least up to the confining pressure of 125 MPa. A calculation with the effective medium theory (Kirkpatrick, 1973) suggests that the fluid forms a network with small coordination number (average coordination number=2.3), and that the connectivity at higher pressures is maintained by stiff pores. More cracks are open at lower pressures to link pores, drastically increasing electrical conductivity.

Keywords: pore, crack, connectivity, granitic rock, electrical conductivity

## Geometry of intergranular fluids in the mantle xenoliths: Implications for the physical properties of upper mantle

NAKAMURA, Michihiko<sup>1\*</sup>; OKUMURA, Satoshi<sup>1</sup>; YOSHIDA, Takeyoshi<sup>1</sup>; SASAKI, Osamu<sup>2</sup>; TAKAHASHI, Eiichi<sup>3</sup>

<sup>1</sup>Graduate School of Science, Tohoku University, <sup>2</sup>Tohoku University Museum, <sup>3</sup>Graduate School of Science and Engineering, Tokyo Institute of Technology

Recent magnetotelluric (MT) studies have revealed that crust and uppermost mantle are less resistive than dry rocks in various localities in the world. This suggests that interconnected fluid phases present more ubiquitously than previously realized. Intergranular fluids also decrease seismic wave velocities and changes Vp/Vs ratio, thus interpretation of the seismic tomographic images largely depends on the volume fraction and geometry of the fluid phase. The conventional view on grain-scale fluid distribution is based on dihedral angle between minerals and fluids in isotropic monomineralic rocks (i.e. ideal equilibrium geometry). Natural rocks are, however, composed of anisotropic multiple phases and undergo textural adjustment to minimize interfacial and strain energy such as grain growth and dynamic recrystallization, which results in microstructural complexity. In order to understand real fluid distribution in deep-seated rocks, we conducted an X-ray CT study of xenoliths from the uppermost mantle from various localities.

The mantle xenolith samples investigated were from Ichinomegata (NE Japan), Eifel (W Germany), San Carlos (AZ, USA), Bullen Merri and Shadwell (Victoria, AU), Kilbourne Hole (New Mexico, USA), Longang-hu (NE China), Gi-rona (Spain), Lanzarote (Canary islands), and Moses Rocks (Uta, USA). The micro-focus X-ray CT imaging was performed using Comscantecno ScanXmate-D160TSS105 in Tohoku University Museum with a tube voltage of 100 – 130 kV and current of 90 – 120 mA. The voxel size was typically 43 – 73  $\mu\text{m}^3$ . The 3-D image analysis was carried out with a software package Slice[1].

All the observed spinel lherzolite and Harzburgite xenoliths contained up to a few vol% of intergranular pores, indicating that the rocks were saturated with a free-fluid phase. The imaged pore fluids are typically polyhedral and tens – hundreds of micrometers in scale; this suggests that they were formed via coalescence of smaller pore fluids. The fluids are localized in interphase boundaries (between different mineral phases), while most of the monomineralic triple junctions lack pore fluids. All these characteristics are consistent with the results of grain-growth experiments in a fluid-bearing bimineralic system[2]; in other words, the role of interfacial energy anisotropy and grain growth are crucial in determining fluid distribution in nature. In the ellipsoid approximation, the 3-D shape of the intergranular fluids show deformed rugby-ball shape with aspect ratios larger than those of the equilibrium fluid geometry determined by the dihedral angle[3]. The geometry, distribution and thus connectivity of fluids cannot be assessed simply from dihedral angles.

The results of CT imaging suggest that no pervasive grain-scale fluid interconnection is established in the uppermost mantle. To explain the observed low electrical resistivity in the mantle which does not undergo partial melting, concentration (localization) and interconnection of CHO fluids in a larger spacing, such as in meter-scale shear zones should be necessary. Given the observed geometry of the inter-granular fluids, their effects on Vp/Vs ratio is limited.

References: [1] Nakano et al. <http://www-bl20.spring8.or.jp/slice/> (2006). [2] T. Ohuchi and M. Nakamura J. Geophys. Res. 111, B01201, doi: 10.1029/2004JB003340 (2005). [3] Y. Takei JGR 107 (B2) doi:10.1029/2001JB000522 (2002).

Keywords: mantle xenoliths, rock microstructure, elastic wave velocity, electrical resistivity, grain growth

## Ultra-fine textures along grain boundaries in nominally fresh mantle xenoliths

MURATA, Masami<sup>1\*</sup> ; UEMATSU, Katsuyuki<sup>2</sup> ; YAMAMOTO, Takafumi<sup>3</sup> ; TANI, Kenichiro<sup>4</sup> ; SHUKUNO, Hiroshi<sup>5</sup> ; MIZUKAMI, Tomoyuki<sup>1</sup> ; MORISHITA, Tomoaki<sup>1</sup>

<sup>1</sup>Kanazawa Univ., <sup>2</sup>Marine Works Japan LTD., <sup>3</sup>Hiroshima Univ., <sup>4</sup>JAMSTEC, <sup>5</sup>non party

It is important for the evolution of the Earth to understand the role of grain boundaries during melts/fluids migrations in mantle peridotites. There are, however, very limited numbers of studies on grain boundaries in natural samples, although many experimental and theoretical approaches have been carried out (e.g., Drury and Fitz Gerald, *Geophys. Res. Lett.*, 1996; Hiraga et al., *Nature*, 2004).

We focus on nanoscale microstructures of crystal surface (grain boundary) in “ nominally fresh ” peridotite xenoliths from the San Carlos, USA, which is one of the most famous localities of peridotite xenolith in the world. Thin amorphous films along grain boundaries were already reported in some San Carlos xenoliths (Wirth, *Contrib. Mineral. Petrol.*, 1996).

We recovered mineral grains with a selfFrag at the Japan Agency for Marine-Earth Science and Technology (JAMSTEC) in order to minimize mechanical damages during mineral separations. We observed multiple grains of peridotite xenoliths using a high-resolution electron microscope (FE-SEM) at JAMSTEC.

Microstructures of crystal surface of these peridotite xenoliths are classified as follows. (1) over micron scale structures such as moth-eaten structures, vermicular structures, automorphic crystals and etch pits. (2) submicron scale structures. It is interesting to note that (2) submicron scale structures are frequently observed on (1) over micron scale structures. These textures suggest that microstructures were developed by several stages. We analysed on the surface of these textures using a micro-Raman and SEM-EDS techniques. We are also planning to perform transmission electron microscope, combined with chemical analyses in order to identify the surface materials that constrain P-T conditions and fluids for the formation of these textures.

Keywords: peridotite xenolith, Microstructures, TEM, grain boundary, fluids

## Elemental transport under lower-middle crustal condition: example from hydration of basic schist, Sanbagawa belt, Japan

UNO, Masaaki<sup>1\*</sup>; NAKAMURA, Hitomi<sup>2</sup>; IWAMORI, Hikaru<sup>3</sup>

<sup>1</sup>Graduate School of Environmental Studies, Tohoku University, <sup>2</sup>Department of Earth and Planetary Sciences, Tokyo Institute of Technology, <sup>3</sup>Geochemical Evolution Research Program, Japan Agency for Marine-Earth Science and Technology

To constrain the behavior of geofluids under the lower to middle crustal conditions, hydration reactions and trace element and Sr-Nd-Pb isotopic compositions of basic schists in the Cretaceous Sanbagawa metamorphic belt, a typical regional metamorphic belt in the circum-Pacific orogeny, have been investigated based on the observations of thin-sections and outcrops. The basic schists have undergone significant hydration from 0.8 GPa, 550 °C to 0.3 GPa, 400 °C during decompression towards the surface at the final stage of metamorphism. High-field-strength and rare-earth element compositions of the basic schists, as well as the Sr-Nd-Pb isotopic ratios, are different among three mineral zones with different peak P-T metamorphic conditions; the basic schists in the low-grade chlorite zone shows N-MORB-like compositions whereas those in the higher-grades, garnet and oligoclase-biotite zones, show more enriched compositions (E-MORB-like). On the other hand, there is a common feature to all the metamorphic zones; the enrichment degree of some group of elements (e.g., large-ion lithophile elements) relative to high-field-strength and heavy-rare-earth elements is proportional to loss on ignition that approximately measures the bulk rock H<sub>2</sub>O content. This correlation suggests that Li, B, K, Cr, Ni, Rb, Sr, Cs and Ba have been added to the basic schists during hydration. The addition of these elements amounts to as much as 60-80% of the bulk abundance, indicating that significant amounts of elements were transported via pervasive fluid flow, which overprinted the variation in the bulk rock compositions of the protolith. The estimated compositions of hydration fluid show high concentrations in large-ion lithophile elements, lead and light-rare-earth elements (10-100 times denser than primitive mantle, Fig. 1) and are similar to those of the slab-derived fluids<sup>[1]</sup> that induce arc volcanism. These elements (Cs, Rb, Ba, K, La, Ce and Pb) are thought to have been preferentially partitioned into the fluid when it was generated at depth. Such high concentrations indicate a high temperature origin of the hydration fluid, and are consistent with a model of hot slab subduction during exhumation of the Sanbagawa belt.

### References:

[1] Nakamura, H., Iwamori, H., and Kimura, J.-I., 2008 *Nat. Geosci.*, **1**, 380-384

Keywords: geofluid, metamorphism, trace elements, Sr-Nd-Pb isotopes, hydration reaction, Sanbagawa metamorphic belt

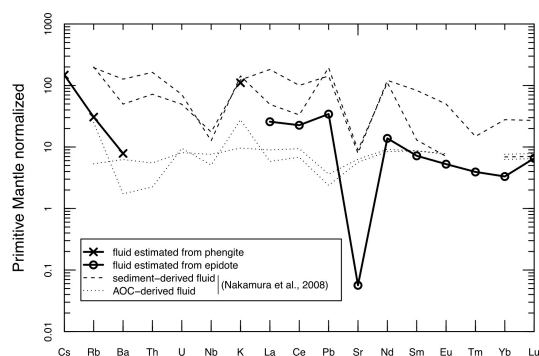


Fig. 1 Estimated compositions of the hydration fluid (solid lines). Compositions of slab-derived fluids estimated for arc volcanism (dotted lines; Nakamura *et al.*, 2008 *Nat. Geosci.*, **1**, 380-384) are shown for comparison. Note that the concentrations of LILE, Pb and LREE in the hydration fluid are in the range of slab-derived fluids.

## Progress of serpentinization in the mantle wedge and its effect on the redox state

KOGISO, Tetsu<sup>1\*</sup> ; MIYOSHI, Akane<sup>2</sup>

<sup>1</sup>Human Environ. Stds., Kyoto Univ., <sup>2</sup>JX Nippon Oil & Energy Corporation

Serpentinization of peridotite in the mantle is a key process that significantly changes the physical properties of the mantle. Serpentinization also produces hydrogen, which is essential not only for the activity of microbial systems in hydrothermal fields on the seafloor, but also for controlling the oxidation state of the mantle in subduction zones. Hydrogen is generated along with the formation of magnetite during serpentinization. However, there still remains controversy about what factors promote the mineralogical reactions responsible for magnetite formation during serpentinization in natural ultramafic rocks. Recent petrologic studies have proposed that serpentinization reactions proceed via a two-stage process involving the early formation of serpentine and brucite and subsequent magnetite formation. Many studies proposed that magnetite forms by the break down of ferrous brucite promoted by the addition of aqueous silica, but others proposed that magnetite forms by the breakdown of ferrous serpentine which releases silica component. To solve this controversy, we examined a number of variably serpentinized harzburgite and dunite samples taken from the Iwanaidake ultramafic body in Kamuikotan belt, Japan (Miyoshi et al. 2014). Petrographic observations of these samples revealed that successive changes in textures, mineral chemistry, whole-rock H<sub>2</sub>O contents, and magnetic susceptibility with the progress of serpentinization of harzburgite involved two stages: replacement of olivine by serpentine and brucite, and subsequent formation of magnetite along with more-magnesian serpentine and brucite. The later reactions occurred concurrently with serpentinization of orthopyroxene, which supplied the silica component. In serpentinized dunite, which doesn't contain orthopyroxene, serpentinization involved replacement of olivine by serpentine and brucite, and the fraction of magnetite did not increase with the progress of serpentinization. These observations, and the fact that the Iwanaidake ultramafic body originated from the forearc mantle of the Northeast Japan arc, suggest that the silica supply from serpentinization of orthopyroxene is an essential factor for the formation of magnetite during serpentinization in mantle wedge.

Our observations imply that serpentinization in the mantle wedge of subduction zone produces H<sub>2</sub> along with magnetite if sufficient amounts of silica component are supplied from subducting slab, which will probably occur because dehydration in subducted sediments can supply silica-rich fluids. Since H<sub>2</sub> is expected to exist as immiscible hydrogen-rich gas phases that coexist with H<sub>2</sub>O fluids in normal subduction zone conditions, it will be rapidly migrate upwards owing to its very low density. Then the remaining serpentinites will become oxidized. Such oxidation associated with serpentinization would occur in the shallow part of the wedge corner where temperatures are lower than ~600 °C, but the oxidized (magnetite-bearing) serpentinite will be dragged downwards in the mantle wedge. Thus serpentinization reactions can be one of the main processes to increase the oxygen fugacity of the mantle wedge. On the other hand, the H<sub>2</sub> gas removed from the wedge corner will produce highly reduced fluid phases, which may result in reducing the shallowest part of the forearc mantle and the lower part of the forearc crust. This could be the cause of rare presence of metal phases in subarc peridotite.

Reference:

A. Miyoshi, T. Kogiso, N. Ishikawa, K. Mibe (2014) *American Mineralogist*, in press.

Keywords: serpentinization, hydrogen, magnetite, subduction zone, redox state

## Evolution of porosity structures in a fracture during quartz vein formation

YAMADA, Ryo<sup>1\*</sup>; OKAMOTO, Atsushi<sup>1</sup>; SAISHU, Hanae<sup>1</sup>; NAKAMURA, Michihiko<sup>2</sup>; OKUMURA, Satoshi<sup>2</sup>; SASAKI, Osamu<sup>3</sup>; TSUCHIYA, Noriyoshi<sup>1</sup>

<sup>1</sup>Tohoku university, <sup>2</sup>Tohoku university, <sup>3</sup>The Tohoku university museum

Ubiquitous occurrences of quartz veins suggest that dissolution/precipitation of silica provides significant effects on the hydrological and mechanical properties within the crust. For example, a model has been proposed that fracture sealing processes control the change of pore fluid pressure and thus earthquake cycle. Previous studies on natural quartz veins have focused on estimates of P-T conditions, stress and strain fields and fluid compositions; however, details of dynamics of fluid flow and how fractures are sealed during vein formation are still unclear. In this study, we synthesized quartz veins by the hydrothermal experiments, and observed the aperture structures by using X-ray CT to clarify how aperture structures evolve during vein formation.

We conducted the hydrothermal flow-through experiments for quartz precipitation from Si-supersaturated solutions under controlled high temperature and high pressure condition. The experimental apparatus consists of two vessels for preparation of the Si-supersaturated solution and for precipitation, respectively. The precipitation vessel has double-structure: the main flow path was the inner alumina tube (diameter=4mm), and the outer SUS tube was filled with static solutions. The advantage of this system is that we can take out the non-destructive sample for the X-ray CT analyses. We conducted two types experiments: first one is precipitation in porous media with alumina balls, the second one is rock slice as analog of a fracture.

In the alumina-ball experiments, we carried out the precipitation experiment at supercritical (430C, 30MPa) and vapor condition (370C, 20MPa). In both experiments, the significant silica precipitation within few days, but showed contrasting porosity structures. Under supercritical condition, amorphous silica was predominantly formed with covering the surfaces of the alumina balls and alumina tube, and discrete quartz crystal (50  $\mu\text{m}$ ) within the amorphous silica layers. The porosity ( $\phi$ ) gradually decreases with minimal porosity ( $\phi = 0.4$ ) at  $\sim 38\text{mm}$  from the inlet. In contrast, under vapor condition, fine-grained quartz grains (0.1-1  $\mu\text{m}$ ) were directly nucleated in solutions using surface of vapor, and immediately settled on the bottom. The porosity rapidly decreases from 18 mm ( $\phi = 0.8$ ) to 25 mm ( $\phi < 0.1$ ) from the inlet. These results suggest that a depressurization of crustal fluids related to fault dilation by earthquakes would cause a formation of fine-grained silica particles, and their mineralogy and transport/deposition properties strongly depend on properties water.

In the experiment with rock slits, we evaluated the effect of rock substrate (amount and distribution quartz in the fracture wall). The P-T conditions and solution chemistry are similar to the previous experiments, but we used granite core with a slit ( $\sim 300 \mu\text{m}$ ). The mineralogy and aperture structures changes systematically along the fluid flow path. From the inlet to 35 mm of fracture, nucleation of quartz and other silica polymorphs predominantly occurred, regardless of vein wall minerals. From  $>35\text{mm}$  low Si concentration, silica precipitates occurred as epitaxial overgrowth from quartz crystal. The wavelength of aperture structures is controlled by distribution and grain size of quartz of the host granite. Accordingly, fractures are not sealed homogeneously, but complex flow pathways are evolved during vein formation. Such a variation in the precipitation mechanism and porosity structures during quartz vein formation may affect the evolutions of permeability and strength of rock fractures in the Earth's crust.

Keywords: Hydrothermal experiments, Quartz, Vein, Fracture, Porosity

## High precision in situ Pb isotope analysis of galena by LAL-ICPMS technique

WAKAKI, Shigeyuki<sup>1\*</sup> ; TANIMIZU, Masaharu<sup>1</sup>

<sup>1</sup>Kochi Institute for Core Sample Research, JAMSTEC

Radiogenic Nd and Pb isotopic compositions of the fluids originated from subducting Pacific and Philippine Sea plates have been characterized from isotopic trends observed among arctic volcanic rocks (Nakamura et al., 2008). Origin and evolution of the fluids that produced hydrothermal ore deposits may now be investigated by radiogenic isotopic compositions of ore deposits. In this study, we analyzed the micro scale isotopic variation of Pb in a hydrothermal galena to shed light on the macro scale dynamics of the fluids. To investigate the possibly small degree of isotopic changes within a galena sample, both high spatial resolution and high precision are required for the isotopic analysis. We employed the combination of laser ablation in liquid (LAL) micro sampling technique (Okabayashi and Hirata, 2011) and solution-based Pb isotopic analysis by MC-ICPMS technique to meet the analytical requirements. In the LAL micro sampling, laser-ablated sample particles are trapped in the liquid that placed above the sampling area. The trapped samples are then dissolved and introduced to the ICPMS as a solution. The advantage of the combined LAL-ICPMS technique over laser ablation (LA) ICPMS technique is the stable ion signals due to solution form, which allows high-precision isotope ratio measurement.

Sample analyzed in this study was a hydrothermal galena from Hosokura mine (Miyagi, Japan). A microscopic texture of the sample was observed in detail with FE-SEM-EDS system (JEOL JSM-6500F) prior to the isotopic analysis. A fs laser (IFRIT, Cyber Laser, Japan) with a wavelength of 780 nm (~200 fs pulse width) was used for the LAL micro sampling. Care was taken to avoid sampling of grain boundaries and inclusions. Typical spatial resolution was 150 micron in diameter and 30 micron in depth. The laser-sampled PbS (300-400ng Pb) trapped in Milli-Q water was dissolved in conc. HNO<sub>3</sub>, and adjusted to 200 ng/mL Pb solution in 0.15 M HNO<sub>3</sub> for Pb isotopic analysis. Pb isotope ratios were determined with a MC-ICPMS, Neptune (Thermo Instruments, Bremen, Germany). An isotopic reference material of Tl (NIST-SRM 997) was added to the final sample solutions for the correction of mass discrimination of Pb in the instrument to have a concentration of 20 ppb Tl.

Galena occurs as discrete layers of ca. 1cm width in between layered CaF<sub>2</sub> as well as sub mm-sized inclusion within thick CaF<sub>2</sub> layer. Galena inclusion and layers were numbered from 1 to 3 according to its precipitation order. Grain size of the galena in each of the layer is several hundred microns to several millimeters. Euhedral quartz with a size of 10-100 micron occurs along the grain boundary of galena and as an inclusion within galena grains.

Small but significant Pb isotopic variation of sub-permil order was observed among and within the 3 galena layers. The analyzed samples clearly form a linear trend in the <sup>208</sup>Pb/<sup>207</sup>Pb vs. <sup>206</sup>Pb/<sup>207</sup>Pb diagram. The observed Pb isotopic trend indicates that the Pb isotopic composition of the fluid that produced the galena has slightly changed during galena precipitation. The Pb isotopic composition of the galena is consistent with mixing of a sediment component of the Pacific plate (Nakamura et al., 2008) with a deep fluid derived from Pacific Ocean plate (Nakamura et al., 2008) and/or the DMM. With the high-precision isotopic analysis as demonstrated in this study, LAL-ICPMS may have an important contribution to high-spatial-resolution geochemical studies in the future.

Keywords: Geofluids, laser ablation in liquid, Pb isotope ratio, galena, in situ isotope analysis

## Origin of saline waters distributed along the Median Tectonic Line in southwest Japan

AMITA, Kazuhiro<sup>1\*</sup> ; OHSAWA, Shinji<sup>2</sup> ; NISHIMURA, Koshi<sup>3</sup> ; YAMADA, Makoto<sup>4</sup> ; MISHIMA, Taketoshi<sup>2</sup> ; KAZAHAYA, Kohei<sup>5</sup> ; MORIKAWA, Noritoshi<sup>5</sup> ; HIRAJIMA, Takao<sup>6</sup>

<sup>1</sup>Department of Earth Science & Technology Faculty of Engineering and Resource Science Akita University, <sup>2</sup>Institute for Geothermal Sciences, Graduate School of Science, Kyoto University, <sup>3</sup>Faculty of Economics, Toyo University, <sup>4</sup>Research Institute for Humanity and Nature, <sup>5</sup>Geological Survey of Japan, AIST, <sup>6</sup>Department of Geology and Mineralogy, Graduate School of Science, Kyoto University

To identify of metamorphic dehydrated fluid as source fluid of hot spring water, we conducted chemical and isotopic analyses of water and accompanied gas samples collected from hot-spring wells along the Median Tectonic Line (MTL) in the forearc region of the southwestern part of Japan. As a result, we found hot spring waters having anomalous dD and d<sup>18</sup>O compositions as compared with modern seawater and shallow groundwater in Wakayama and Shikoku regions. Judging from data in relative B-Li-Cl composition and He isotopic systematics, the source fluid of the hot springs in Shikoku could be identified to be one of diagenetic fluids. On the other hand, the source fluid of the hot springs of Wakayama had different B-Li-Cl composition and higher 3He/4He ratio in comparison with diagenetic dehydrated fluids and then the fluid was thought to be originated from metamorphic dehydrated fluid as well as Oita plain. There was another striking contrast between the source fluid of Wakayama and Oita and that of Shikoku and Miyazaki; accompanied gases by the former were rich in CO<sub>2</sub>, whereas those with the latter were rich in CH<sub>4</sub>, and CO<sub>2</sub> in the accompanied gases of Wakayama and Oita is mostly derived from marine carbonate like volcanic gases in subduction zones. Moreover, the Li-B-Cl compositions of them showed transitive values between the relative composition of diagenetic fluids and those of volcanic thermal waters. Consequently, the source fluid of hot springs in Wakayama and Oita was likely to be dehydrated metamorphic fluids released from the subducting Philippine-Sea plate.

Keywords: hot spring water, dehydrated fluid from subducting plate, Median Tectonic Line

## Distribution of the helium isotope ratios in northeast Japan in terms of geological setting

HORIGUCHI, Keika<sup>1\*</sup> ; KAZAHAYA, Kohei<sup>1</sup> ; TSUKAMOTO, Hitoshi<sup>1</sup> ; MORIKAWA, Noritoshi<sup>1</sup> ; SATO, Tsutomu<sup>1</sup> ; OHWADA, Michiko<sup>1</sup> ; NAKAMA, Atsuko<sup>1</sup>

<sup>1</sup>Geological Survey of Japan, AIST

The distribution of slab fluid defined by high Li/Cl ratios conforms the area of "hot fingers" (Tamura et al., 2002) in Northeast Japan (Kazahaya et al., submitted). Conversely, the high <sup>3</sup>He/<sup>4</sup>He ratios distribute wider and do not match with slab-derived fluids indicating that some of the mantle-derived helium would not be transported with magmas or slab fluids but directly upwells as mantle-derived fluid. The <sup>3</sup>He/<sup>4</sup>He ratios vary along the volcanic front showing an areal contrast; such as a low-ratio-area close to volcanoes are observed in the central part of Tohoku. We propose here an extended helium upwell model which can explain the spatial variation of <sup>3</sup>He/<sup>4</sup>He ratios with the following concept; 1) The most important constraint for mantle helium upwelling is the crustal structure divided by tectonic lines; Hatagawa Tectonic Line (HTL) divides the Kitakami and Abukuma belts. Ryoke belt and north part of Abukuma belt is torn apart by number of faulting events. The rest of parts, Abukuma granitic province and Kitakami province form very large stable blocks which might prohibit helium to upwell from mantle. 2) A view from U-Th content in the crust is important to understand the flat distribution of mantle helium in back-arc region; Low U-Th crust in the back-arc with less crustal <sup>4</sup>He production is favorable to explain the flat and high <sup>3</sup>He/<sup>4</sup>He signature, such as oceanic crust might have. Tanakura Tectonic Line (TTL) divides the thick crust of continental margin (sedimentary prism and granite) with Ryoke belt.

Keywords: helium isotope ratio, northeast Japan, areal distribution, geological structure

## The Li-Cl-Br systematics of saline groundwater: A new indicator for slab fluid

KAZAHAYA, Kohei<sup>1\*</sup>; TAKAHASHI, Masaaki<sup>1</sup>; IWAMORI, Hikaru<sup>2</sup>

<sup>1</sup>Geological Survey of Japan, AIST, <sup>2</sup>Geochemical Evolution Research Program, Japan Agency for Marine-Earth Science and Technology

In this study, we propose Br/Cl ratio as a new indicator for slab-derived fluids, which is useful to distinguish their sources between pore water and hydrous minerals in subducting slab. The areal distribution of slab-derived fluids and their sources using Li/Cl and Br/Cl as geochemical evidences will provide a view for water circulation in subduction zones.

Subducting slab contains waters (originally seawater) as pore water and many kinds of hydrous minerals. Hydrous minerals such as opal, clay or mica will decompose to release water during subsiding, and pore water will be released by compaction. Even though such complex process occurs, behavior of halogen ions in the subducting slab may be simple because they are always enriched in aqueous phase (pore water) and the rest are in minerals as a replacement of OH. Some metamorphic fluids in wedge mantle peridotite with Br-enriched signature have been observed and were indicated to be from pore water in the slab. The mineral dehydration process is supposed to be responsible for Br-depletion in slab-derived aqueous fluid. Therefore, halogens are potentially good indicators concerning with the water behavior in subduction processes.

The higher Br/Cl ratios (>0.0035 in wt.) have been observed in fossil seawater and oil field brines due to the addition of Br from organic matters. The very low Br/Cl waters (<0.0025 in wt.) have feature of <sup>18</sup>O-shift to the slab (magmatic) fluid end member, which is quite lower than that in seawater (Br/Cl = 0.0034 in wt.), indicating that these waters originate from dehydration of the slab.

Keywords: Li-Cl-Br, slab-derived fluid, groundwater, subduction process

## Origin of U-Th disequilibrium in subduction zone volcanic rocks

YOKOYAMA, Tetsuya<sup>1\*</sup>; IKEMOTO, Akihiko<sup>1</sup>; IWAMORI, Hikaru<sup>2</sup>; UEKI, Kenta<sup>1</sup>

<sup>1</sup>Department of Earth and Planetary Sciences, Tokyo Institute of Technology, <sup>2</sup>JAMSTEC

Subduction zone magmatism is induced by the addition of slab derived fluids to the mantle wedge [1]. Chemical compositions of subduction zone volcanic rocks are largely controlled by the chemical and physical properties of the slab fluid. The nature of slab fluids have been extensively studied by geochemical approach utilizing trace element abundances and isotope compositions in arc basalts [2]. U-series disequilibrium in arc volcanic rocks is a useful tracer to understand the origin of arc magmas as well as the timescales of fluid/melt migration in subduction zones. However, detail of the process that producing <sup>238</sup>U-<sup>230</sup>Th disequilibrium in primary melts in the mantle wedge is still poorly constrained.

In this study, we determined <sup>238</sup>U-<sup>230</sup>Th disequilibrium in volcanic rocks from the Northeast Japan Arc (Iwate, Akitakoma, Yakeyama, Hachimantai, and Kampu). In addition, we performed a numerical simulation that reproduced (<sup>238</sup>U/<sup>232</sup>Th) and (<sup>230</sup>Th/<sup>232</sup>Th) ratios in primary melts in a subduction zone, by simultaneously calculating mantle dynamics, hydro phase reactions and trace elements transport. To discuss the origin of U-Th disequilibrium in arc volcanic rocks, the new data and previously published U-Th data around Japan were evaluated based on the result of the numerical simulation. The numerical simulation performed in this study

Most of arc volcanic rocks possess <sup>238</sup>U-<sup>230</sup>Th disequilibrium with <sup>238</sup>U excesses, suggesting the addition to the mantle wedge of slab fluid enriched in U relative to Th. The feature of <sup>238</sup>U enrichment is well reproduced by the numerical simulation. Interestingly, the simulation produced two positive trends in the U-Th diagram; the shallow trend matches data from the Izu-Mariana arc, while the steep slope is consistent with data from the Kamchatka arc. This strongly suggests that the positive trend in the U-Th diagram for a single arc samples simply reflects the variation of (<sup>238</sup>U/<sup>232</sup>Th) and (<sup>230</sup>Th/<sup>232</sup>Th) ratios in primary melts produced in the mantle wedge, and the slope does not have any age significance. Thus, as discussed in [3], the decoupling of U-Th and Th-Ra ages for arc samples would be explained by assuming that the slab derived fluid have (<sup>230</sup>Th/<sup>232</sup>Th) ratios higher than the mantle wedge composition.

Although the NEJ frontal-arc lavas (Iwate) possess <sup>238</sup>U-<sup>230</sup>Th disequilibrium with <sup>238</sup>U excesses, the extent of <sup>238</sup>U enrichment is moderate (<10%) compared to the other frontal-arc samples. In addition, Iwate lavas have relatively low (<sup>230</sup>Th/<sup>232</sup>Th) ratios that cannot be explained by the numerical simulation. This implies that the (<sup>230</sup>Th/<sup>232</sup>Th) in mantle wedge beneath Iwate volcano is lower than that in the depleted MORB mantle (DMM), due presumably to ancient mantle metasomatism by Th-enriched fluids derived from sediments.

In contrast to the frontal arc samples, the extent of <sup>238</sup>U enrichment in the NEJ samples decreases as the slab depth increases, and the rear-arc lavas (Kampu) show <sup>230</sup>Th enrichments relative to <sup>238</sup>U (<10%). This generally reflects gradual decrease of the amount of slab derived fluid mixed into the wedge mantle. The <sup>230</sup>Th excesses in rear-arc lavas would be produced by the melting of garnet-bearing upwelling mantle, as reproduced by the simulation. However, our data for Kampu show <sup>230</sup>Th excesses with an extremely low (<sup>230</sup>Th/<sup>232</sup>Th) ratio (~0.8) that plots outside the simulation data. This is explained by assuming the existence of metasomatised mantle beneath the NE Japan as discussed above, although the possibility of direct addition of Th-enriched fluid to the DMM-like mantle cannot be ruled out for the generation of rear-arc magmas.

References: [1] Iwamori (1998) *EPSL* 160, 65. [2] Nakamura et al. (2008) *Nature Geosci.* 1 380. [3] Yokoyama et al. (2003) *JGR* doi: 10.1029/2002JB002103.

Keywords: U-Th disequilibrium, Subduction zone, volcanic rocks, slab derived fluid

## Water transport coupled dynamically with a plate-mantle convection system involving a shallow to deep subduction zone

NAKAKUKI, Tomoeki<sup>1\*</sup>; KANEKO, Takeo<sup>1</sup>; NAKAO, Atsushi<sup>2</sup>; IWAMORI, Hikaru<sup>3</sup>

<sup>1</sup>Dept. Earth and Planetary Systems Science, Hiroshima Univ., <sup>2</sup>Dept. Earth and Planetary Sciences, Tokyo Inst. Technology, <sup>3</sup>Geochemical Evolution Research Program, JAMSTEC

Numerical study for water transport under a volcanic arc revealed dynamics of the water processes inducing melt generation (Iwamori, 1998; 2007). Back-arc and intra-plate volcanisms also indicate water migration from a deeper section of the subduction zone. Aiming to understand geodynamical processes of water derived and transported from the subducted slab in the deep subduction zone, we developed a numerical model of water transport coupled dynamically with plate-mantle convection system with a whole mantle scale. We here focus on the mechanism of dehydration from stagnating or penetrating slab and water transport from the mantle transition zone (MTZ). We also consider water transport to deeper mantle and the effects on the global distribution of water-compatible elements (Iwamori and Nakamura, 2012).

We assume that a viscous fluid in a 2-D rectangular box with an extended Boussinesq approximation represents the mantle convection system with integrated lithospheric plates (Tagawa et al, 2007). We incorporate water transport and hydrous mineral phase diagram (Iwamori, 1998; 2007) into the numerical plate-mantle model. We assume that the water dehydrated from water-saturated minerals migrates upward with porous flow that is much faster than mantle flow. In our model, the emitted water is instantaneously transported only to the upward direction. We introduce reduction of the density and the viscosity due to the hydration into the density and rheology model according to experimental study (karato and Jung, 2003). We also consider viscous weakening of serpentine or chlorite that is important for water transport in shallow subduction zone [6]. A numerical method developed by Tagawa et al. (2007) is used to solve momentum and energy conservation equations for the mantle convection. To solve an equation for water transport advected by the mantle flow in which the diffusion term is negligible, a Marker-And-Cell (MAC) method is employed to avoid artificial diffusion.

A serpentine layer generated by dehydration of the oceanic crust plays a key role to control water transport by the subducted slab shallower than about 150 km (Iwamori, 1998; 2007; Horiuchi, 2013). To continuously generate this layer, coupling between the serpentine layer and the plate boundary fault is essential. After dehydration of serpentine, nominally anhydrous minerals (NAMs) (Iwamori, 1998; 2007) are a main veneer of the water. In this stage, water capacity of NAMs, which depends on the grain boundary storage as well as that of the hydrous minerals, is the primary factor to control the amount of transported water. This is not so large as about 0.4 wt. % to maintain water-filled region under the arc. The water is carried without dehydration above the 660 km boundary. If the water capacity in the lower mantle is as large as that of NAMs in the mantle shallower than 410 km (~0.2 wt. %), the water is entirely transported to the lower mantle. When the lower mantle water capacity is lower than that, the water is expelled at the post-spinel phase transition. While the water ascends with the porous flow, the medium rocks descend with asthenospheric flow dragged by the downwelling slab. The repetition of these processes broadens the hydrous layer at the 660 km boundary. A thin water-saturated layer is formed at the 660 km boundary around the penetrating slab. Because of the buoyancy, this becomes unstable so that hydrous plumes are generated. On the contrary to this, the hydrous plume was not formed from the hydrous NAMs layer over the stagnant slab. At the 410 km boundary, the water is ejected from the hydrous plume as the olivine phase minerals can bear the water much less than MTZ minerals. The ejected water rises with porous flow till the emission is completed. The hydrous plumes fill the water within the mantle wedge from the edge to the 500 to 1000 km distant back-arc area, and those erode to thin the overriding lithosphere.

Keywords: subduction zone, water transport, transition zone, slab, hydrous plume, mantle convection